THE EUROPEAN
PHYSICAL JOURNAL C

Different critical points of chiral and deconfinement phase transitions in (2 + 1)-dimensional fermion–gauge interacting model

Hong-tao Feng[1,4,a], **Feng-yao Hou**[2,4], **Yong-hui Xia**[3], **Jun-yi Wang**[3], **Hong-shi Zong**[3,4,b]

[1] Department of Physics, Southeast University, Nanjing 211189, China
[2] Institute of Theoretical Physics, CAS, Beijing 100190, China
[3] Department of Physics, Nanjing University, Nanjing 210093, China
[4] State Key Laboratory of Theoretical Physics, Institute of Theoretical Physics, CAS, Beijing 100190, China

Abstract Based on the truncated Dyson–Schwinger equations for fermion and massive boson propagators in QED$_3$, the fermion chiral condensate and the mass singularities of the fermion propagator via the Schwinger function are investigated. It is shown that the critical point of the chiral phase transition is apparently different from that of the deconfinement phase transition and in Nambu phase the fermion is confined only for small gauge-boson mass.

1 Introduction

The chiral and deconfinement phase transitions of nonperturbative systems are important issues of continuous interests both theoretically and experimentally. Although the mechanism is unknown, the originally chiral symmetric system may undergo chiral phase transition (CPT) into a phase with dynamical chiral symmetry breaking (DCSB) which explains the origin of the constituent-quark masses in QCD and underlies the success of chiral effective field theory [1,2]. In the chiral limit, the order parameter of CPT is defined via the fermion propagator

$$\langle \bar{\psi} \psi \rangle = \text{Tr}[S(x \equiv 0)] = \int \frac{\mathrm{d}^d p}{(2\pi)^d} \frac{4B(p^2)}{A^2(p^2)p^2 + B^2(p^2)}. \tag{1}$$

The two functions $A(p^2)$ and $B(p^2)$ in the above equation are related to the inverse fermion propagator

$$S^{-1}(p) = i\gamma \cdot p A(p^2) + B(p^2). \tag{2}$$

The deconfinement phase transition is then related to the observation of the free particle and also the corresponding

[a] e-mail: fenght@seu.edu.cn

[b] e-mail: zonghs@chenwang.nju.edu.cn

propagator. If the full fermion propagator has no mass singularity in the timelike region, it can never be on mass shell and the free particle can never be observed where the confinement happens [3]. Accordingly, the appearance of the mass singularity in the system directly implies deconfinement. So in this way we can learn as regards the deconfinement phase transition from the analytic structure of the fermion propagator.

To indicate DCSB and confinement, it is very suggestive to study some model that reveals the general nonperturbative features while being simpler. Three-dimensional quantum electrodynamics (QED$_3$) is just such a model which has many features similar to quantum chromodynamics (QCD), such as DCSB and confinement [2–5]. Moreover, its super-renormalization obviates the ultraviolet divergence which is present in QED$_4$. For these reasons, it can serve as a toy model of QCD. In parallel with its relevance as a tool through which to develop insight into aspects of QCD, QED$_3$ is also found to be equivalent to the low-energy effective theories of strongly correlated electronic systems. Recently, QED$_3$ has been widely studied in graphene [6–8] and high-T$_c$ cuprate superconductors [9–12].

The study of DCSB in QED$_3$ has been an active research subject for nearly 30 years, since Appelquist et al. [13] found that DCSB vanishes when the flavor of the massless fermions reaches a critical number $N_c \approx 3.24$. They gained this conclusion by solving the truncated Dyson–Schwinger equation (DSE) for the fermion propagator in the chiral limit. Later, extensive analytical and numerical investigations showed that the existence of DCSB in QED$_3$ remains the same after including higher order corrections to the DSE [14,15]. On the other hand, the achievement in the research of the mass singularity and confinement in QED$_3$ is caused by a paper of Maris [3] who found that the fermion is confined by the truncated DSE for the full fermion and boson propagators at $N < N_c$ where chiral symmetry is broken. This result might

imply that the existence of confinement and DCSB depends on the same boundary conditions. Moreover, the authors of Refs. [2,16] pointed out that restoration of chiral symmetry and deconfinement are coincident owing to an abrupt change in the analytic properties of the fermion propagator when a nonzero scalar self-energy becomes insupportable.

Nevertheless, the above result will be altered when the gauge boson acquires a finite mass ζ through the Higgs mechanism [17,18], or from a topological origin [19,20]. For a fixed $N(< N_c)$ and with the increasing boson mass, the fermion chiral condensate falls and diminishes at a critical value ζ_c (which, of course, depends on N) and then chiral symmetry is restored. Since DCSB and confinement are nonperturbative phenomena, both of them occur in the low-energy region and might disappear with the increase of the boson mass. Therefore, it is very interesting to investigate whether or not both phase transitions occur at the same critical point in this case. One may argue that, with the introduction of the explicit photon mass term, the potential obtained from the full photon propagator will be attended at long distance, and the potential is no longer confining. Here, it is of heuristic interest to compare this case with that of QCD, where the quark interacts via the gluons. Lattice simulations illustrate that the gluon has a nonzero mass at zero temperature and zero density where, because of the occurrence of confinement, the free quarks cannot be observed [21]. This indicates that the nonzero mass of the boson *does not* destroy confinement. Based on the same spirit in this paper, we aim to adopt the truncated DSEs for the full propagators to study the behaviors of the mass singularity and the fermion chiral condensate with a range of gauge-boson mass and try to answer this question.

2 Schwinger function

The Lagrangian for massless QED$_3$ in a general covariant gauge in Euclidean space can be written as

$$\mathcal{L} = \bar{\psi}(\slashed{\partial} - i e \slashed{A})\psi + \frac{1}{4}F_{\sigma\nu}^2 + \frac{1}{2\xi}(\partial_\sigma A_\sigma)^2, \tag{3}$$

where the 4-component spinor ψ is the massless fermion field, ξ is the gauge parameter. This system has chiral symmetry and the symmetry group is $U(2)$. The original $U(2)$ symmetry reduces to $U(1) \times U(1)$ when the massless fermion acquires a nonzero mass due to nonperturbative effects. Just as mentioned in Sect. 1, the chiral symmetry is broken by the dynamical generation of the fermion mass (here $N = 1$). Since the earlier work shows that the Schwinger function is suitable for the description of the fermion mass as regards the axiom of reflection positivity. Note that the Schwinger function with oscillatory behavior is not positive definite, which is an easily identifiable signal in $\Omega(t)$ due to the pair of complex conjugate poles. This violates the axiom of reflection

positivity. It follows from this that an oscillating behavior of the function describes a field with a complex mass spectrum and/or residues that are not positive. This is appropriate for particles that decay and forms the basis of the argument that such a propagator allows a state to exist only for a finite time before stabilization; i.e., that the propagator describes a confined fermion [22]. If one adopts the full boson propagator, the results of the Euclidean-time Schwinger function reveal that the fermion propagator has a complex mass singularity and thus corresponds to a nonphysical observable state [3], which means the appearance of confinement. On the contrary, if the Schwinger function exhibits a real mass singularity of the propagator, the fermion is observable and the fermion is not confined [24,25]. Therefore, we also adopt this method to analyze those nonperturbative phenomena.

The Schwinger function can be written as

$$\Omega(t) = \int d^2\vec{x} \int \frac{d^3p}{(2\pi)^3} e^{i(p_0 t + \vec{p}\cdot\vec{x})} \frac{M(p^2)}{p^2 + M^2(p^2)} \tag{4}$$

with $M(p^2) = B(p^2)/A(p^2)$. If there are two complex conjugate mass singularities $m^* = a \pm ib$ associated with the fermion propagator, the function will show an oscillating behavior,

$$\Omega(t) \sim e^{-at}\cos(bt + \phi), \tag{5}$$

for large (Euclidean) t.

However, if the system reveals a stable observable asymptotic state with a mass m for the fermion propagator, then

$$\Omega(t) \sim e^{-mt} \Rightarrow \lim_{t\to\infty} \ln\Omega(t) \sim -mt. \tag{6}$$

In this way, the analysis of the mass singularity can be used to determine whether or not the fermion is confined. Since the Schwinger function is determined by the fermion propagator and the DSEs provide us a powerful tool to study it, we shall use the coupled gap equations to calculate this function.

3 Truncated DSE

Now let us turn to the calculation of $A(p^2)$ and $B(p^2)$. These functions can be obtained by solving DSEs for the fermion propagator,

$$S^{-1}(p) = S_0^{-1}(p) + \int \frac{d^3k}{(2\pi)^3}[\gamma_\sigma S(k)\Gamma_\nu(p, k)D_{\sigma\nu}(q)], \tag{7}$$

where $\Gamma_\nu(p, k)$ is the full fermion–photon vertex and $q = p - k$. The coupling constant $\alpha = e^2$ has dimension one and provides us with a mass scale. For simplicity, in this paper temperature, mass, and momentum are all measured in units of α, namely, we choose a kind of natural units in which $\alpha = 1$. From Eqs. (2) and (7), we obtain the equation satisfied by $A(p^2)$ and $B(p^2)$:

$$A(p^2) = 1 - \frac{1}{4p^2} \int \frac{\mathrm{d}^3 k}{(2\pi)^3} \mathrm{Tr}[i(\gamma p)\gamma_\sigma S(k)\Gamma_\nu(p,k)D_{\sigma\nu}(q)],$$
(8)

$$B(p^2) = \frac{1}{4} \int \frac{\mathrm{d}^3 k}{(2\pi)^3} \mathrm{Tr}[\gamma_\sigma S(k)\Gamma_\nu(p,k)D_{\sigma\nu}(q)].$$
(9)

Another involved function $D_{\sigma\nu}(q)$ is the full gauge-boson propagator which is given by [17,18]

$$D_{\sigma\nu}(q) = \frac{\delta_{\sigma\nu} - q_\sigma q_\nu/q^2}{q^2[1 + \Pi(q^2)] + \zeta^2} + \xi \frac{q_\sigma q_\nu}{q^4},$$
(10)

where $\Pi(q^2)$ is the vacuum polarization for the gauge boson which is satisfied by the polarization tensor

$$\Pi_{\sigma\nu}(q^2) = - \int \frac{\mathrm{d}^3 k}{(2\pi)^3} \mathrm{Tr}[S(k)\gamma_\sigma S(q+k)\Gamma_\nu(p,k)], \quad (11)$$

and ζ is the gauge-boson mass which is acquired through the Higgs mechanism which happens when the gauge field interacts with a scalar field in the phase with spontaneous gauge symmetry breaking (here, we adopt the massive boson propagator to investigate the oscillation behavior of Schwinger function in DCSB phase; more details as regards the Higgs mechanism in QED$_3$ can be found in Refs. [17,23]).

Using the relation between the vacuum polarization $\Pi(q^2)$ and $\Pi_{\sigma\nu}(q^2)$,

$$\Pi_{\sigma\nu}(q^2) = (q^2 \delta_{\sigma\nu} - q_\sigma q_\nu)\Pi(q^2),$$
(12)

we can obtain an equation for $\Pi(q^2)$ which has an ultraviolet divergence. Fortunately, it is present only in the longitudinal part and is proportional to $\delta_{\sigma\nu}$. This divergence can be removed by the projection operator

$$\mathcal{P}_{\sigma\nu} = \delta_{\sigma\nu} - 3\frac{q_\sigma q_\nu}{q^2},$$
(13)

and then we obtain a finite vacuum polarization [4,5].

Finally, we choose to work in the Landau gauge, since the Landau gauge is the most convenient and commonly used one. Once the fermion–boson vertex is known, we immediately obtain the truncated DSEs for the fermion propagator and then analyze the deconfinement transition and CPT in this Higgs model.

3.1 Rainbow approximation

The simplest and most commonly used truncated scheme for the DSEs is the rainbow approximation,

$$\Gamma_\nu \to \gamma_\nu,$$
(14)

since it gives us rainbow diagrams in the fermion DSE and ladder diagrams in the Bethe–Salpeter equation for the fermion–antifermion bound state amplitude. In the framework of this approximation, the coupled equations for mass-

less fermion and massive boson propagators reduce to the three coupled equations for $A(p^2)$, $B(p^2)$, and $\Pi(q^2)$,

$$A(p^2) = 1 + \int \frac{\mathrm{d}^3 k}{(2\pi)^3} \frac{2A(k^2)(pq)(kq)/q^2}{p^2 G(k^2)[q^2(1 + \Pi(q^2)) + \zeta^2]},$$
(15)

$$B(p^2) = \int \frac{\mathrm{d}^3 k}{(2\pi)^3} \frac{2B(k^2)}{G(k^2)[q^2(1 + \Pi(q^2)) + \zeta^2]},$$
(16)

$$\Pi(q^2) = \int \frac{\mathrm{d}^3 k}{(2\pi)^3} \frac{2A(k^2)A(p^2)}{q^2 G(k^2)G(p^2)}$$
$$\times [2k^2 - 4(k \cdot q) - 6(k \cdot q)^2/q^2],$$
(17)

with $G(k^2) = A^2(k^2)k^2 + B^2(k^2)$. By the application of iterative methods, we can obtain A, B, and Π.

3.2 Improved scheme for DSE

To improve the truncated scheme for DSE, there are several attempts to determine the functional form for the full fermion–gauge-boson vertex [26–30], but none of them completely resolves the problem. However, the Ward–Takahashi identity,

$$(p - k)_\nu \Gamma_\nu(p,k) = S^{-1}(p) - S^{-1}(k),$$
(18)

provides us an effectual tool to obtain a reasonable ansatz for the full vertex [31]. The portion of the dressed vertex which is free of kinematic singularities, i.e. the BC vertex, can be written as

$$\Gamma_\nu(p,k) = \frac{A(p^2) + A(k^2)}{2}\gamma_\nu + \frac{B(p^2) - B(k^2)}{p^2 - k^2}(p+k)_\nu$$
$$+ (\not{p} + \not{k})\frac{A(p^2) - A(k^2)}{2(p^2 - k^2)}(p+k)_\nu.$$
(19)

Since the numerical results obtained using the first part of the vertex coincide very well with earlier investigations [15], we choose this one as a suitable ansatz,

$$\Gamma_\nu^{\mathrm{BC}_1}(p,k) \simeq \frac{1}{2}[A(p^2) + A(k^2)]\gamma_\nu,$$
(20)

to be used in our calculation. Following the procedure in the rainbow approximation, we also obtain the three coupled equations for $A(p^2)$, $B(p^2)$, and $\Pi(q^2)$ in the improved truncated scheme for DSEs,

$$A(p^2) = 1 + \int \frac{\mathrm{d}^3 k}{(2\pi)^3} \frac{A(k^2)[A(p^2) + A(k^2)](pq)(kq)/q^2}{p^2 G(k^2)[q^2(1 + \Pi(q^2)) + \zeta^2]},$$
(21)

$$B(p^2) = \int \frac{\mathrm{d}^3 k}{(2\pi)^3} \frac{[A(p^2) + A(k^2)]B(k^2)}{G(k^2)[q^2(1 + \Pi(q^2)) + \zeta^2]},$$
(22)

$$\Pi(q^2) = \int \frac{\mathrm{d}^3 k}{(2\pi)^3} \frac{A(k^2)A(p^2)[A(p^2) + A(k^2)]}{q^2 G(k^2)G(p^2)}$$
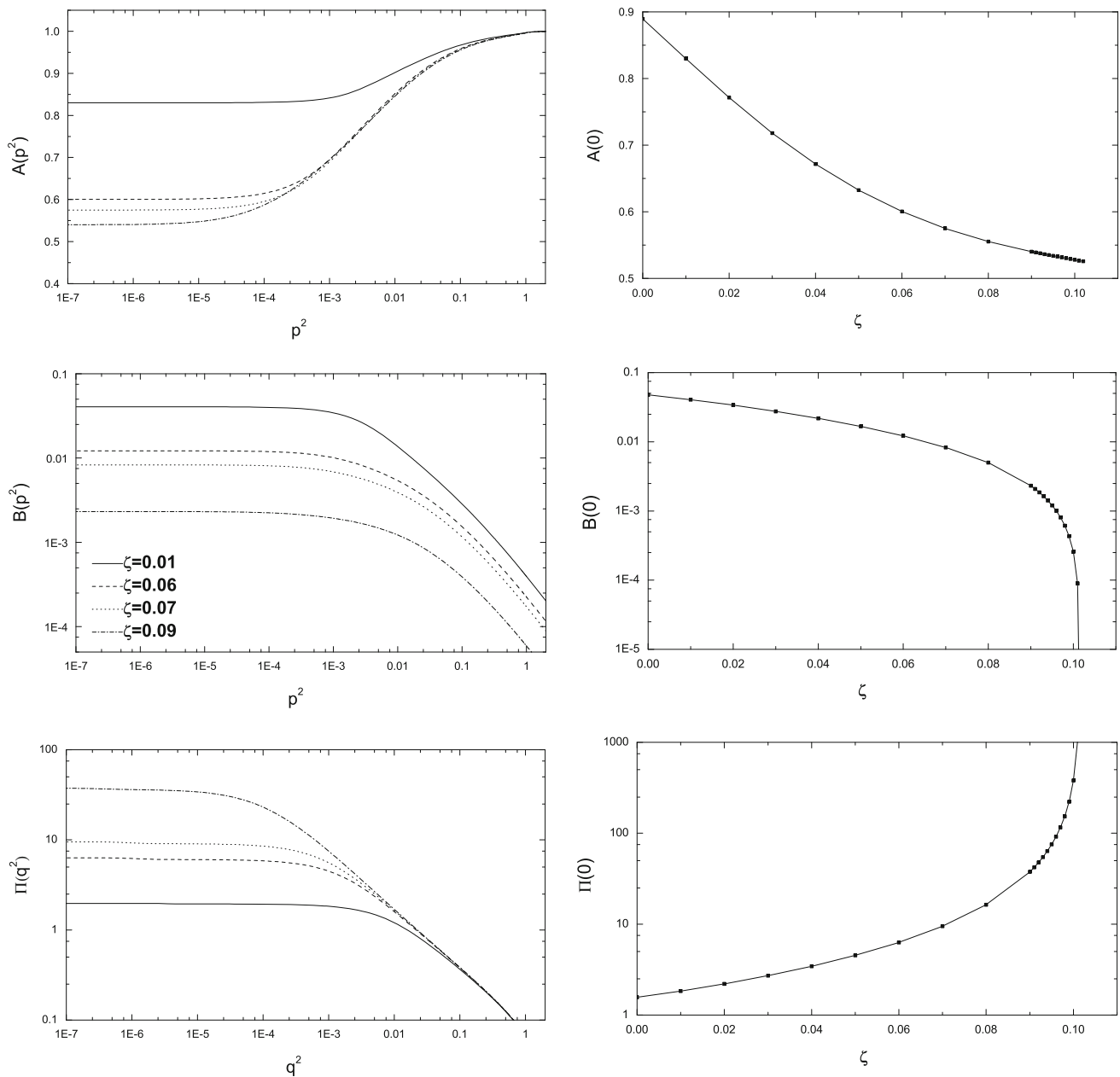$$\times [2k^2 - 4(k \cdot q) - 6(k \cdot q)^2/q^2].$$
(23)

Fig. 1 The typical behaviors of $A(p^2)$, $B(p^2)$, $\Pi(q^2)$ (*left*) and their infrared values (*right*) as functions of the boson mass in DCSB phase

4 Numerical results

After solving the above coupled DSEs in the rainbow approximation by means of the iteration method, we can obtain the three functions A, B, Π for the propagator and plot them in Fig. 1.

From Fig. 1 it can be seen that $A(p^2)$ increases with increasing momenta but is almost equal to one at large p^2. In the range of small momenta, it decreases but does not vanish when $p^2 \to 0$. Both of the other two functions, $B(p^2)$ and $\Pi(q^2)$, decrease at large momenta but their rates of decreas-

ing are different. $B(p^2)$ decreases as rapidly as $\sim 1/p^2$, while $\Pi(q^2)$ decreases as rapidly as $\sim 1/\sqrt{q^2}$. In addition, all the three functions are constant in the infrared region. Thus, we can obtain the values of the corresponding functions A, B, and Π at zero momenta, which, as functions of the gauge-boson mass ζ, are also shown in Fig. 1. As ζ increases, both $A(0)$ and $B(0)$ decrease, and $B(0)$ vanishes when ζ reaches a critical gauge-boson mass $\zeta_c^R \approx 0.102$, whereas the function $\Pi(0)$ increases and diverges at the same critical boson mass ζ_c^R. Based on Eq. (1), the critical boson mass can be regarded as the point of CPT.
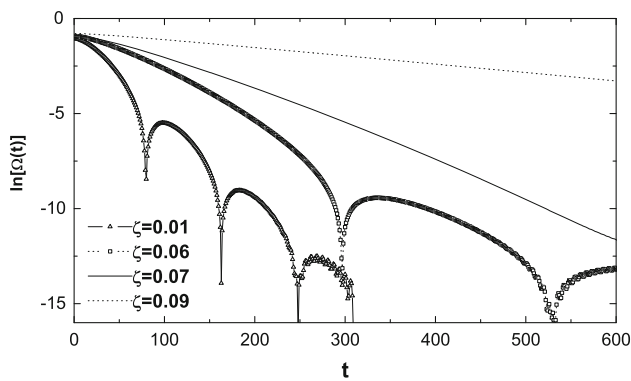
Fig. 2 Logarithm of the absolute value of the Schwinger function with several ζ for the rainbow approximation

Then, substituting the obtained A and B into Eq. (4), we immediately obtain the behavior of the Schwinger function with nonzero boson mass which is shown in Fig. 2. At small ζ, the Schwinger function reveals its typical oscillating behavior, which illustrates the conjugate mass singularities like $m^* = a \pm ib$

$$m^* \sim 0.043 \pm 0.063i \text{ at } \zeta = 0.01, \tag{24}$$
$$m^* \sim 0.023 \pm 0.025i \text{ at } \zeta = 0.06, \tag{25}$$

associated with the fermion propagator; thus the free particle can never be observed where the fermion is confined. On the increase of ζ, the oscillating behavior remains but it vanishes at another critical value $\zeta_{dc}^R \approx 0.068$ and around it both of the propagators do not exhibit any singularity.

Beyond ζ_{dc}^R, the function $\ln[\Omega(t)] \sim -mt$ where the stable asymptotic state of the fermion is observable,

$$m \approx 0.021 \text{ at } \zeta = 0.07, \tag{26}$$
$$m \approx 0.0041 \text{ at } \zeta = 0.09, \tag{27}$$

and hence the deconfinement phase transition happens, but the DCSB remains. With the enlargement of ζ, the absolute slope of $\ln[\Omega(t)]$ decreases and m disappears at ζ_c^R.

To validate the difference between ζ_c and ζ_{dc}, we also give the behavior of the Schwinger function beyond the rainbow approximation in Fig. 3. In the BC_1 truncated scheme for DSE, the oscillation of the Schwinger function only appears at small ζ, which denotes the existence of confinement, but it disappears at $\zeta_{dc}^{BC_1} \approx 0.038$, which exhibits that the deconfinement phase transition occurs but here $\langle \bar{\psi}\psi \rangle \neq 0$. On the increase of ζ, the Schwinger function shows the real mass singularity of the propagator and chiral symmetry gets restored when the boson mass reaches $\zeta_c^{BC_1} \approx 0.071$.

Moreover, we investigate the critical behaviors with a range of $N (< N_c)$. Our numerical results show that, whereas each of the two critical value changes with N, the qualitative conclusion that ζ_c is larger than ζ_{dc} remains.
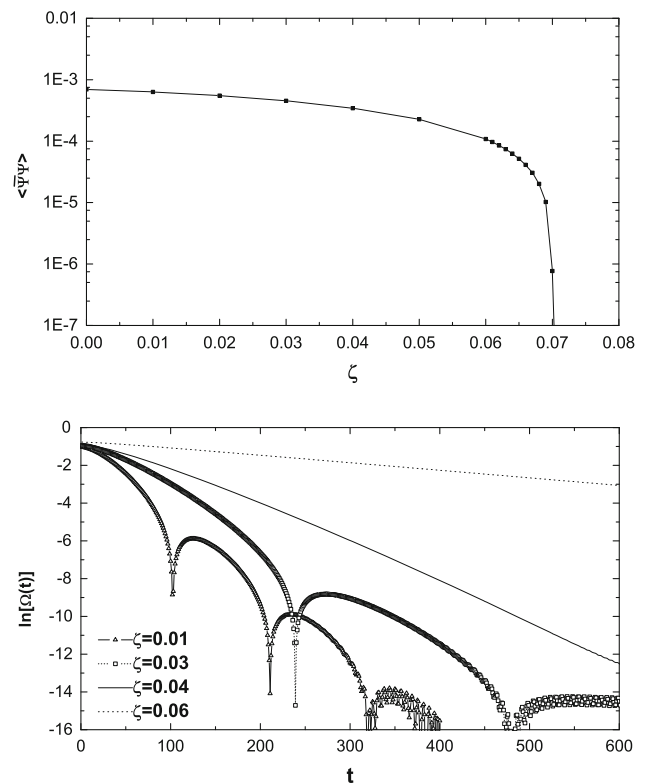

Fig. 3 The value of fermion chiral condensate (*top*) and the logarithm (*bottom*) in the framework of BC_1 vertex with a range of ζ

5 Conclusions

The primary goal of this paper is to investigate the chiral and the deconfinement phase transition by application of an Abelian Higgs model through a continuum study of the Schwinger function. Based on the rainbow approximation of the truncated DSEs for the fermion propagator and numerical model calculations, we study the behavior of the Schwinger function and the fermion chiral condensate. It is found that, with the increase of the gauge-boson mass, the vanishing point (ζ_{dc}) of the oscillation behavior of the Schwinger function is apparently less than that of the fermion chiral condensate and each of the propagators *does not* reveal any singularity near ζ_{dc}. To understand the difference between the two critical points, we also work in an improved scheme for the truncated DSEs and show that the above conclusion remains despite the fact that the two critical numerical values are altered. The result indicates that, with the increasing gauge-boson mass in the chiral model, the occurrence of the deconfinement phase transition is apparently earlier than that of the chiral phase transition.

References

1. C.D. Roberts, Prog. Part. Nucl. Phys. **61**, 50 (2008)
2. A. Bashir, A. Raya, I.C. Cloet, C.D. Roberts, Phys. Rev. C **78**, 055201 (2008)
3. P. Maris, Phys. Rev. D **52**, 6087 (1995)
4. N. Brown, M.R. Pennington, Phys. Rev. D **39**, 2723 (1989)
5. C.J. Burden, J. Praschifka, C.D. Roberts, Phys. Rev. D **46**, 2695 (1992)
6. D.V. Khveshchenko, Phys. Rev. Lett. **87**, 246802 (2001)
7. V.P. Gusynin, S.G. Sharapov, Phys. Rev. Lett. **95**, 146801 (2005)
8. J.E. Drut, T.A. Lahde, Phys. Rev. Lett. **102**, 026802 (2009)
9. N. Dorey, N.E. Mavromatos, Nucl. Phys. B **386**, 614 (1992)
10. M. Franz, Z. Tesanovic, O. Vafek, Phys. Rev. B **66**, 054535 (2002)
11. W. Rantner, X.G. Wen, Phys. Rev. B **66**, 144501 (2002)
12. P.A. Lee, N. Nagaosa, X.G. Wen, Rev. Mod. Phys. **78**, 17 (2006)
13. T. Appelquist, D. Nash, L.C.R. Wijewardhana, Phys. Rev. Lett. **60**, 2575 (1988)
14. D. Nash, Phys. Rev. Lett. **62**, 3024 (1989)
15. C.S. Fischer, R. Alkofer, T. Dahm, P. Maris, Phys. Rev. D **70**, 073007 (2004)
16. C.P. Hofmann, A. Raya, S.S. Madrigal, Phys. Rev. D **82**, 096011 (2010)
17. G.Z. Liu, G. Cheng, Phys. Rev. D **67**, 065010 (2003)
18. H.T. Feng, W.M. Sun, F. Hu, H.S. Zong, Int. J. Mod Phys. A **20**(13), 2753 (2005)
19. S. Deser, R. Jackiw, S. Templeton, Ann. Phys. **140**, 372 (1982)
20. J.F. Schonfeld, Nucl. Phys. B **185**, 157 (1981)
21. O. Oliveira, P. Bicudo, J. Phys. G Nucl. Part. Phys. **38**, 045003 (2011)
22. C.D. Roberts, A.G. Williams, Prog. Part. Nucl. Phys. **33**, 477 (1994)
23. J.F. Li, H.T. Feng, Y. Jiang, W.M. Sun, H.S. Zong, Mod. Phys. Lett. A **27**, 1250026 (2012)
24. L.C.L. Hollenberg, C.D. Roberts, B.H.J. McKellar, Phys. Rev. C **46**, 2057 (1992)
25. C.D. Roberts, A.G. Williams, Prog. Part. Nucl. Phys. **33**, 477 (1994)
26. D.C. Curtis, M.R. Pennington, Phys. Rev. D **42**, 4165 (1990)
27. M.R. Pennington, D. Walsh, Phys. Lett. B **253**, 246 (1991)
28. K.-I. Kondo, P. Maris, Phys. Rev. Lett. **74**, 18 (1995)
29. G.W. Semenoff, P. Suranyi, L.C.R. Wijewardhana, Phys. Rev. D **50**, 1060 (1994)
30. P.M. Lo, E.S. Swanson, Phys. Rev. D **83**, 065006 (2011)
31. J.S. Ball, T.W. Chiu, Phys. Rev. D **22**, 2542 (1980)